Integrated analysis of FANCE expression and its regulatory role in the immune microenvironment of oral squamous cell carcinoma

BO LIN[1-4], YULING CHEN[1-4], XIAOLIAN LI[1-4], YUNTAO LIN[1-4], JIAN ZHOU[1-4], HONGYU YANG[1-4] and YUEHONG SHEN[1-4]

[1]Department of Oral and Maxillofacial Surgery, Stomatological Center, Peking University Shenzhen Hospital, Shenzhen, Guangdong 518036, P.R. China; [2]Department of Oral and Maxillofacial Surgery, Guangdong Provincial High-level Clinical Key Specialty, Shenzhen, Guangdong 518036, P.R. China; [3]Department of Oral and Maxillofacial Surgery, Guangdong Province Engineering Research Center of Oral Disease Diagnosis and Treatment, Shenzhen, Guangdong 518036, P.R. China; [4]Institute of Stomatology, Shenzhen Clinical Research Center for Oral Diseases, Peking University Shenzhen Hospital, Shenzhen Peking University-The Hong Kong University of Science and Technology Medical Center, Shenzhen, Guangdong 518036, P.R. China

Received July 2, 2024; Accepted December 6, 2024

DOI: 10.3892/ol.2025.14906

Abstract. Oral squamous cell carcinoma (OSCC) presents a significant health challenge owing to its complex origin and limited treatment success. The precise function of Fanconi anemia complementation group E (FANCE), a key gene involved in DNA repair in OSCC, remains unclear. The present study performed bioinformatics analysis of The Cancer Genome Atlas dataset and cellular experiments to demonstrate that FANCE is significantly upregulated in OSCC. Enhanced FANCE expression was associated with poor survival outcome in patients with OSCC. Knockdown of FANCE inhibited OSCC cell proliferation and migration. Moreover, a negative correlation was observed between FANCE expression and immune cell markers. Collectively, these findings suggest that FANCE is a potential oncogene in OSCC and a prognostic biomarker that may play a role in modulating the OSCC microenvironment.

Introduction

Head and neck cancers, particularly oral squamous cell carcinoma (OSCC), pose a significant global health challenge owing to the complex etiology and limited success of treatment for improving patient survival (1). Intricate interplay among genetic alterations, environmental exposure and viral infections has been implicated in the pathogenesis of OSCC. However, the precise molecular mechanisms underlying their development have not been fully elucidated (2). This underscores the need for innovative investigations to identify novel molecular targets that aid the development of effective therapeutics.

Based on the molecular landscape, Fanconi anemia complementation group E (FANCE) has been identified as a key component of DNA damage response mechanisms, particularly in the Fanconi anemia (FA) pathway, where it plays a vital role in repairing DNA interstrand crosslinks and maintaining genomic stability (3,4). FANCE primarily functions in the repair of DNA interstrand crosslink-complex forms of DNA damage that, if not properly repaired, can lead to genomic instability and elevate the risk of cancer development (5). By effectively repairing these interstrand crosslinks, FANCE not only safeguards the integrity of the genetic material of the cell but also contributes to the maintenance of a stable genomic environment, which is crucial for cellular health and the prevention of malignancies (3). Emerging evidence suggests that FANCE may also influence the tumor microenvironment (TME) through mechanisms beyond its canonical DNA repair functions, potentially affecting immune responses within the tumor (6). This dual role of FANCE, not only in maintaining genomic stability but also in possibly modulating immune activity, raises intriguing questions about its broader impact on tumor progression and therapeutic resistance in OSCC (7). These considerations underscore the importance of further research to explore how FANCE may contribute to both the oncogenic processes and the modulation of the tumor immune microenvironment in OSCC, which could reveal new avenues for targeted therapy and prognostic assessment.

The expression of FANCE is aberrant in various types of cancer (6,8,9), including head and neck squamous cell carcinoma (HNSCC). Altered expression of FANCE has been linked to a five-year survival rate in patients with HNSCC, suggesting its potential use as a prognostic biomarker (6). In

Correspondence to: Professor Hongyu Yang or Dr Yuehong Shen, Department of Oral and Maxillofacial Surgery, Stomatological Center, Peking University Shenzhen Hospital, 1120 Lianhua Road, Futian, Shenzhen, Guangdong 518036, P.R. China
E-mail: hyyang192@hotmail.com
E-mail: yuehongshen@hotmail.com

Key words: oral squamous cell carcinoma, Fanconi anemia complementation group E, biomarker, prognosis, tumor microenvironment

addition, epigenetic modifications, such as changes in methylation patterns, have been associated with aberrant FANCE expression in these malignancies (10). Furthermore, FANCE expression is associated with immune cell infiltration, particularly by $CD4^+$ T cells and macrophages, indicating its potential involvement in modulating the tumor immune microenvironment (6,7).

The present study aimed to determine the function of FANCE in the development of OSCC by assessing its expression profiles and association with immune markers, as well as its functional implications for tumor cell biology. Furthermore, the association between FANCE and immune markers was explored to understand its potential influence on the tumor immune microenvironment. This comprehensive approach allowed investigation into how FANCE may modulate both oncogenic processes and immune responses in OSCC. The findings of the present study could provide valuable insights into the molecular mechanisms underlying OSCC progression and potentially inform the development of novel targeted therapeutic strategies and prognostic assessments.

Material and methods

Data acquisition and preprocessing. Gene expression data and clinical information for OSCC were retrieved from The Cancer Genome Atlas (TCGA, cancer.gov/tcga/) via the Genomic Data Commons Data Portal (https://portal.gdc.cancer.gov/). HNSCC data from TCGA, including RNA-Seq and corresponding clinical metadata, were pre-processed to ensure quality and consistency, (portal.gdc.cancer.gov/projects/TCGA-HNSC). Such processes comprised normalizing expression, removing batch effects and verifying sample annotations using RStudio software v. 3.5.3 (RStudio, Inc.). $P<0.05$ was considered statistically significant.

Differential expression and survival. Differential expression was analyzed to compare FANCE gene expression between normal and OSCC tissue samples from TCGA-HNSC and identify significant changes. The association between FANCE expression and patient survival was assessed using Kaplan-Meier estimates, with log-rank tests for statistical comparison. The analysis was performed with RStudio v. 3.5.3 (RStudio, Inc.); $P<0.05$ was considered statistical significance.

Unsupervised clustering and validation. The optimal number of clusters for patient stratification was identified using the Elbow method (11), which evaluates within-cluster sums of squares to ascertain the point of diminishing returns in cluster variance. Thereafter, patient data, which came from TCGA-HNSC expression profile, were categorized using the k-means clustering algorithm, which is a machine learning technique that partitions data based on inherent gene expression profiles. The resulting clusters were validated using principal component analysis (PCA) to ensure robust separation of the data into distinct genetic profiles (12). Analysis was performed using RStudio v. 3.5.3 (RStudio, Inc.), with $P<0.05$ regarded as statistical significance.

Differential expression in clusters and immune infiltration assessment. To explore the expression profile of FANCE across clusters identified by the Elbow method and categorized using the k-means clustering algorithm during unsupervised learning, unpaired t-tests were used to compare FANCE expression. This comparison aimed to assess the variability in FANCE expression across distinct molecular subtypes, thereby laying the groundwork for further biological interpretation. Having established significant differences in FANCE expression, the underlying biological mechanisms were investigated. The ESTIMATE algorithm was used to quantify and contrast the immune and stromal components of the TME across clusters. This analysis was instrumental in elucidating the potential associations between the differential expression of FANCE and the characteristics of the TME within varying subtypes. Analysis was performed with RStudio v. 3.5.3 (RStudio, Inc.), where $P<0.05$ was taken as the criterion for statistical significance.

Cross-validation of macrophage abundance. The abundance of macrophages within the TME was cross-validated using an array of computational methodologies. Marker gene-based single-sample Gene Set Enrichment Analysis (ssGSEA) enrichment and analyses using MCP-counter (version 1.2.0) and xCell (version 1.1.0), together with the deconvolution algorithms, CIBERSORT (version v1.03) and TIMER (version 2.17), by RStudio v. 3.5.3 (RStudio, Inc.), facilitated a comprehensive assessment of immune cell infiltration within clusters obtained by the Elbow method and k-means clustering. These diverse bioinformatics tools enabled a more nuanced quantitation of macrophage presence and their potential impact on the OSCC microenvironment. $P<0.05$ as the benchmark for statistical significance.

Cell culture and transfection. Human oral keratinocytes (HOKs) were obtained from Shanghai Meixuan Biological Science and Technology Ltd (cat. no. MXC1005). The HSC3 and HN6 cells were obtained from the BeNa Culture Collection (Beijing Beina Chunglian Institute of Biotechnology; cat. no. BNCC341400) and central laboratory of Peking University School of Stomatology, respectively. SCC9 (cat. no. CRL-1629) and SCC25 (cat. no. CRL-1628) cells were purchased from the American Type Culture Collection. The cell lines were incubated at 37˚C under a humidified 5% CO_2 atmosphere in DMEM (Gibco; Thermo Fisher Scientific, Inc.), supplemented with 10% fetal bovine serum and 1% penicillin/streptomycin (all from Gibco; Thermo Fisher Scientific, Inc.). The cell lines were authenticated by short tandem repeat profiling analysis and were free of mycoplasma contamination. FANCE was knocked down in HSC3 and HN6 cells using siRNA (100 nM) transfection with Lipofectamine® 3000 (Thermo Fisher Scientific, Inc.). Following culture at 37˚C for 48 h, the knockdown efficiency of the cells was detected and subsequent experiments were conducted. The siRNA sequences used for FANCE knockdown and the control siRNA were as follows: Negative control-sense: 5'-UUCUCCGAACGUGUCACGUTT-3'; antisense: 5'-ACGUGACACGUUCGGAGAATT-3'; FANCE siRNA-sense: 5'-GCUUCUUCACGAAUGUAGUCC-3'; and antisense: 5'-ACUACAUUCGUGAAGAAGCUG-3'. Control siRNA and siRNA targeting FANCE were purchased from Shanghai GenePharma Co., Ltd.

Reverse transcription-quantitative PCR (RT-qPCR). The mRNA expression of FANCE in HSC3 and HN6 cell lines was assessed by RT-qPCR. Total RNA was extracted from cells using TRIzol® (Takara Bio Inc.), and its integrity was verified by measuring absorbance at 260/280 nm. Complementary DNA was synthesized from 1 μg RNA using the Evo M-MLV RT *Kit* Mix for qPCR [Accurate Biotechnology (Hunan) Co., Ltd.], according to the manufacturer's instructions. RT-qPCR was performed in triplicate using SYBR Green [Accurate Biotechnology (Hunan) Co., Ltd.] under the following cycling conditions: Denaturation at 95˚C for 10 min, then 40 cycles of 95˚C for 5 s and 58˚C for 30 s. Melting curves were analyzed to confirm the product specificity and FANCE mRNA was quantified using the $2^{-\Delta\Delta Cq}$ method (13) with the following forward and reverse (5'3') primers:

FANCE forward, AGGAGAGACCCGAACATAAGTC and reverse: CTCGCCAGTCTTAACTGCCA;

β-actin forward: AAACTGGAACGGTGAAGGTG and reverse: AGTGGGGTGGCTTTTAGGAT, and normalized to β-actin.

Cell proliferation. Cell proliferation was quantified using a cell counting kit-8 (CCK-8; Shenzhen Aipno Biomedical Technology Co., Ltd.). Briefly, cells were seeded at a density of $3x10^3$ cells/well in 96-well plates and left to adhere overnight. The CCK-8 solution was added to the wells at 0, 24, 48 and 72 h after seeding and incubated at 37˚C for 1 h. Absorbance was measured at 450 nm using a microplate reader. Blank readings were subtracted from all measurements.

Wound healing. HSC3 and HN6 cells with FANCE knockdown at 100% confluence were scratched, and adherent cells were rinsed and cultured in serum-free medium. Images of cell migration were captured at various intervals thereafter using inverted fluorescence microscopy (Leica Camera, Germany; DMi8), and wound area was used to measure with image J (1.48v), the ratio of wound closure was calculated. Wound healing rate=(initial area-healing area)/initial area.

Transwell migration. HSC3 ($4x10^4$ cells/well) and HN6 ($6x10^4$ cells/well) with FANCE knockdown suspended in serum-free DMEM were seeded into the upper chamber of Transwell chambers (cat. no. 3422; Corning, Inc.), and DMEM containing 10% FBS was added to the lower chamber, incubated at 37˚C for 24 h, then fixed with 4% paraformaldehyde at room temperature for 30 min and stained with 0.1% crystal violet at room temperature for 30 min. Cells on the surface of the upper membrane were removed, while those on the lower surface were analyzed. Images were acquired under an inverted fluorescence microscopy (Leica, DMi8, Germany) and analyzed using image J (1.48v).

Gene set enrichment analysis. To elucidate the immunological impact of FANCE expression in OSCC, Gene Set Enrichment Analysis (GSEA) was performed. This analysis was executed using the clusterProfiler package within RStudio v. 3.5.3 (RStudio, Inc.), where gene sets were analyzed for differential expression between high and low FANCE-expressing OSCC samples. Significance was determined via phenotype-based permutation tests, with an FDR threshold of 0.25 for identifying notable gene sets. Visual representations were constructed with enrichplot and patchwork, offering a clear depiction of the enrichment results.

FANCE-immune checkpoint correlation analysis. To assess the association between FANCE expression and immune checkpoint genes, RNA sequencing data were assessed from the TCGA OSCC cohort. The expression levels of FANCE and immune checkpoint genes (PD1, PDL1, CTLA4, LAG3, HAVCR2 and TIGIT) were extracted and subjected to statistical analysis using Pearson correlation coefficient. Scatter plots were generated using ggplot2 in RStudio v. 3.5.3 (RStudio, Inc.) to visualize the association between FANCE and the immune checkpoint markers. Statistical significance for all correlations was evaluated with P-values calculated, with $P<0.01$ considered significant.

Immunohistochemical (IHC) staining. The present study involved pathological sections from 13 patients (9 male and 4 female; mean age, 55.62 years; age range, 36-80 years) obtained from the Department of Pathology at Peking University Shenzhen Hospital (Shenzhen, China) between January 2020 and December 2023. The specimens were selected (inclusion criteria of age between 18 and 85 years and pathologically diagnosed as oral squamous cell carcinoma to represent a diverse patient demographic and ensure the relevance of the present findings to the broader OSCC population, while excluding those with severe sample quality problems affecting subsequent staining and patients having other major interfering diseases or a history of special treatments and other unstated factors. Human sample collection was approved by The Ethical Committee of The Peking University Shenzhen Hospital (Shenzhen, China; approval no. 2023-177) and written informed consent was obtained from all participants. Fresh OSCC samples were obtained from the operating room and fixed in 10% neutral buffered formalin for 72 h at room temperature, dehydrated in gradient alcohol solution (50, 70, 80, 95, 95 and 100 alcohol, each for 1 h) and paraffin embedded. Paraffin embedded tumor sections with a thickness of 4 μm were deparaffinized with xylene I for 15 and xylene II for 10 min, and rehydrated with 100, 100, 95, 95 and 80% ethanol for 5 min each. Sections were then washed twice for 5 min each with dH2O. Slides were heated in a microwave in citrate antigen retrieval solution (cat. no. MVS-0066; MBX Bioscience) or TRIS-EDTA antigen retrieval solution (cat. no. BL617A; Biosharp Biotechnology) until boiling (100˚C), followed by incubation at the boiling state for 20 min. After cooling, sections were washed in PBS three times for 5 min each. Antigen retrieval was achieved by blocking with 3% H_2O_2 for 30 min at room temperature. Blocking was performed using 10% goat serum (cat. no. ZLI-9022; ZSGB-BIO) at room temperature for 20 min. The slices were incubated with primary antibody at 4˚C overnight. The following primary antibodies: Anti-FANCE (1:400; cat. no. GTX110184; GeneTex, Inc.) anti-CD68 [1:200; cat. no. 76437; Cell Signaling Technology, Inc. (CST)], anti-CD14 (cat. no. ZA-0532; ZSGB Biotech, Beijing, China) and anti-CD206 (1:400; CST; cat. no. 91992). The slices were incubated with (cat. no. KIT-9710; MBX Biosciences) biotin-labeled goat anti-mouse/rabbit IgG at room temperature

for 10 min, and then incubated with streptomyces peroxidase at room temperature for 10 min. The washing step was repeated, the slices were stained using DAB (cat. no. DAB-1031; MBX Biosciences), and the reaction was aborted with dH2O. The slices were counterstain with hematoxylin at room temperature for 2 min. Stained sections were visualized using a BX53 fluorescence microscope (Olympus Corporation) and analyzed using Image J (1.48v; National Institutes of Health).

Statistical analysis. All data were analyzed using GraphPad Prism 5.0 (Dotmatics) and RStudio software (v. 3.5.3). The R packages used included 'DESeq2', 'survival', 'kmeans', 'factoextra', 'MCPcounter', 'xCell', 'CIBERSORT', 'TIMER', 'ggplot2', 'dplyr', 'tidyr', 'purrr', 'stringr' and 'reshape2'. Data were presented as the mean ± standard deviation. All assays were repeated in at least three independent experiments. $P<0.05$ were considered to indicate a statistically significant difference. Significance was assessed using an unpaired two-tailed Student's t-test for two-group comparisons, Kaplan-Meier method with log-rank tests for survival analysis and Pearson correlation coefficient for correlation analyses.

Results

FANCE expression is upregulated in patients with OSCC. RNA expression (fold-change >2.0; $P<0.05$) and the clinical features of 315 patients with OSCC derived from TCGA database were analyzed to determine the function of FANCE. Table I summarized the clinical features of patients with OSCC. The expression of FANCE was significantly higher in the tumor tissues compared with the normal tissues (Fig. 1A), and was positively associated with T classification and clinical stage (Fig. 1B and C). However, no significant statistical differences in FANCE expression were found in other clinical parameters, such as N classification, perineural invasion or lymphovascular invasion, as detailed in Table II. The results of the Kaplan-Meier curves revealed a correlation between enhanced FANCE expression and poor survival among the patients with OSCC (Fig. 1D). The upregulation of FANCE expression in tumor tissues was also validated by the IHC staining (Fig. 1E). Thus, enhanced FANCE expression was associated with larger tumors, advanced clinical stage and poor survival in patients with OSCC. The expression data of FANCE and the clinical information of the cases are provided in Tables SI and II, respectively.

Integrated cluster analysis of patients with OSCC. The flowchart of bioinformatics analysis of the OSCC dataset are shown in Fig. 2. Integrated cluster analysis of the samples of patients with OSCC revealed distinct gene expression profiles within the dataset. Employing the elbow method, the optimal number of clusters was determined to be two (k=2), as visualized in Fig. 3A, where the total within-cluster sum of squares reached an inflection point. K-means clustering analysis further segregated the OSCC samples into two subgroups: Cluster 1 (n=174) and Cluster 2 (n=141). Principal component analysis (PCA) demonstrated the first two components accounted for 11.3 and 8.3% of the total observed variance, respectively, with the PCA plot exhibiting distinct yet slightly overlapping gene expression profiles for the two clusters as depicted in Fig. 3B. The expression level of the FANCE gene was found to be significantly different between the two clusters. As shown in the box plot (Fig. 3C), Cluster

Table I. Basic information of patients with oral squamous cell carcinoma in the head and neck squamous cell carcinoma dataset.

Clinical parameter	n
Location	315
Alveolar ridge	18
Buccal mucosa	22
Floor of mouth	62
Hard palate	7
Lip	3
Oral cavity	73
Oral tongue	130
Clinical T stage	307
T1	19
T2	100
T3	76
T4	112
Clinical N stage	303
N0	165
N1	56
N2	80
N3	2
Clinical M stage	300
M0	298
M1	2
Clinical stage	307
I	12
II	76
III	65
IVA	154
Lymphovascular invasion	234
No	164
Yes	70
Margin status	302
Close	35
Negative	230
Positive	37
Histological grade	311
G1	49
G2	196
G3	66
Perineural invasion present	247
No	112
Yes	135
Recurrence	277
No	199
Yes	78

Table II. Comparative analysis of FANCE expression in patients with oral squamous cell carcinoma.

Clinical characteristic	n[a]	Median difference[b]	P-value
Alcohol use (no vs. yes)	308	-0.113	0.403
Smoking (no vs. yes)	315	0.029	0.633
N classification (N0 vs. N+)	271	0.061	0.301
T classification (T1 & T2 vs. T3 & T4)	297	-0.303	0.001
Stage (I & II vs. III & IV)	293	-0.239	0.010
Histological grade (G1 and G2 vs. G3)	311	0.212	0.161
Perineural invasion (negative vs. positive)	247	0.022	0.502
Lymphovascular invasion (negative vs. positive)	234	0.049	0.977
Recurrence (no vs. yes)	277	0.006	0.691
Outcome (alive vs. dead)	315	-0.208	0.132

[a]Analyses were conducted on available data. Cases with missing data were excluded from the respective analysis. [b]Median difference reflects the difference in the median expression levels of FANCE between the two comparison groups. FANCE, Fanconi anemia complementation group E.

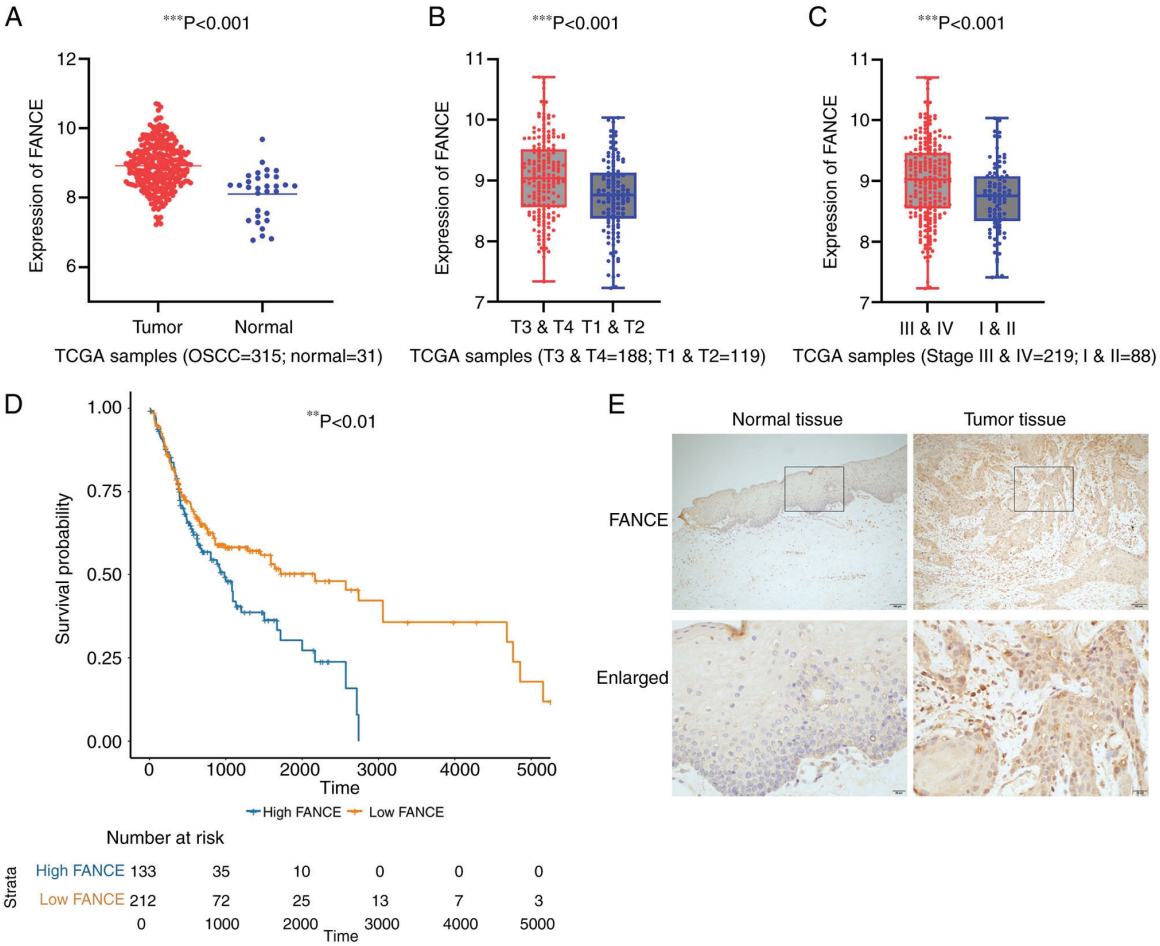

Figure 1. FANCE is upregulated in OSCC. FANCE expression in OSCC and normal tissue samples according to (A) sample types, (B) tumor size (T classification) and (C) tumor clinical stage. Statistical analysis was performed using the two-tailed unpaired student's t-tests, and data are presented as the mean ± SD (***P<0.001). (D) Kaplan-Meier survival analysis of TCGA-OSCC cohorts grouped by FANCE expression level, with statistical comparison performed using the log-rank test. (**P<0.01). (E) IHC staining of FANCE expression in OSCC and normal tissue samples, performed in triplicate (scale bar, 100 and 20 μm, respectively). OSCC, oral squamous cell carcinoma; FANCE, Fanconi anemia complementation group E; TCGA, The Cancer Genome Atlas.

1 had a higher mean FANCE gene expression (9.038±0.595) compared with Cluster 2 (8.787±0.690), with the differences being statistically significant (P<0.05). For detailed FANCE expression data by cluster, see Table SIII. Further comparative

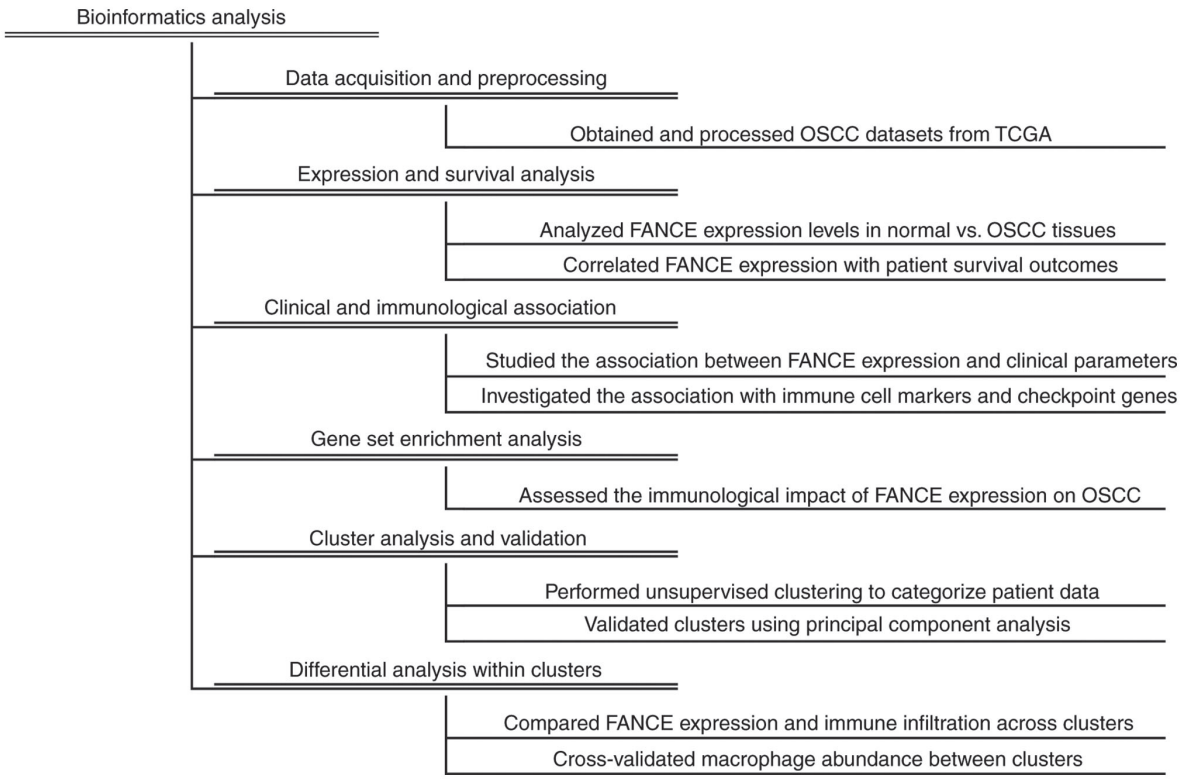

Figure 2. Flowchart of bioinformatic analysis. FANCE, Fanconi anemia complementation group E; TCGA, The Cancer Genome Atlas; OSCC, oral squamous cell carcinoma.

analysis of the TME using the ESTIMATE algorithm revealed notable disparities between the clusters. Cluster 1 presented with a universally lower mean (± SD) stroma, immune and ESTIMATE scores (-675.062±534.185, 307.954±701.403, and -367.108±1117.081, respectively) compared with Cluster 2 (233.293±695.683, 623.624±802.598 and 856.917±1353.531, respectively), with these differences reaching statistical significance ($P<0.05$; Fig. 3D). Furthermore, the macrophage profile of each cluster was assessed using multiple algorithms, including MCP-counter, xCell, CIBERSORT and TIMER. Macrophages were significantly more abundant in Cluster 2, as consistently indicated by all applied algorithms. This is depicted in Fig. 3E-H, where the macrophage abundance scores of the TIMER algorithm were significantly higher for Cluster 2 compared with Cluster 1. Both M0 and M2 macrophages were substantially more prevalent in Cluster 2, while M1 macrophages were observed to be more abundant in Cluster 1, as detailed in the CIBERSORT analysis (Fig. 3F). The MCP-counter analysis also demonstrated a significantly higher monocyte lineage score in Cluster 2 (Fig. 3G). Moreover, xCell algorithm-based analysis revealed a significantly increased abundance of macrophages, including both M1 and M2 subsets, in Cluster 2 (Fig. 3H), highlighting a distinct profile of macrophage infiltration in this subgroup.

Knockdown of FANCE inhibits cell proliferation and migration in OSCC cells. The expression of FANCE in OSCC cells was validated by RT-qPCR. The mRNA expression of FANCE was significantly enhanced in SCC25, SCC9, HN6 and HSC3 cells compared with HOK cells; FANCE expression was enhanced by 1.3- and 1.8-fold in HN6 and HSC3 cells, respectively, compared with HOK cells (Fig. 4A). The elevated expression of FANCE in OSCC cells indicated its potential oncogenic role in oral carcinogenesis. FANCE expression was knocked down in HSC3 and HN6 cells by siRNA transfection and its efficiency was confirmed by RT-qPCR to further analyze FANCE function in OSCC. Knockdown of FANCE significantly inhibited its mRNA expression in HSC3 and HN6 cells by ~65% compared with the control. (Fig. 4B).

The effects of FANCE knockdown on cell proliferation were determined using CCK-8 assays and revealed significantly inhibited proliferative ability compared with controls, and the wound healing rates of knockdown HSC3 and HN6 cells were also decreased (Fig. 4C and D). Knocking down FANCE inhibited HSC3 and HN6 cell migration in Transwell assays by 50 and 30%, respectively, compared with controls (Fig. 4E). Overall, these findings indicate that FANCE expression is upregulated in OSCC cells and that its knockdown inhibits their proliferation and migration.

FANCE expression modulates the OSCC microenvironment. GSEA analysis revealed that FANCE expression is intricately linked to the OSCC TME, particularly in its regulatory effects on immune pathways (Table III). FANCE may act to suppress certain immune pathways under normal conditions, with its reduced expression potentially leading to the activation of these pathways (14), as indicated by negative enrichment scores in gene sets related to systemic lupus erythematosus and asthma. This indicates a dynamic role for FANCE in modulating the immune response within the TME.

FANCE expression showed significant negative correlations with multiple immune checkpoint genes in OSCC,

Table III. Gene set enrichment analysis results of immune-related gene sets in oral squamous cell carcinoma.

Gene sets	Normalized enrichment score	Adjusted P-value
Malaria	-0.806	<0.001
Primary immunodeficiency	-0.794	<0.001
Systemic lupus erythematosus	-0.794	<0.001
Asthma	-0.793	<0.001
Allograft rejection	-0.765	<0.001
Viral protein interaction with cytokine and cytokine receptor	-0.761	<0.001
Graft-vs.-host disease	-0.759	<0.001
African trypanosomiasis	-0.753	<0.001
Intestinal immune network for IgA production	-0.751	<0.001
Hematopoietic cell lineage	-0.730	<0.001
Type I diabetes mellitus	-0.728	<0.001
Autoimmune thyroid disease	-0.722	<0.001
Rheumatoid arthritis	-0.722	<0.001
Inflammatory bowel disease	-0.698	<0.001
Cardiac muscle contraction	-0.695	<0.001
Renin-angiotensin system	-0.682	0.002
Hypertrophic cardiomyopathy	-0.679	<0.001
Leishmaniasis	-0.678	<0.001
Antigen processing and presentation	-0.677	<0.001
Dilated cardiomyopathy	-0.675	<0.001

including programmed Cell Death 1), CD274 (Programmed Death-Ligand 1), CTLA4, LAG3 (Lymphocyte-Activation Gene 3), HAVCR2 (Hepatitis A Virus Cellular Receptor 2) and TIGIT (T cell immunoglobulin and ITIM domain). Scatter plots demonstrated these negative correlations, with Pearson correlation coefficients and corresponding P-values indicating statistical significance for each association (Fig. 5A). Further analysis of TCGA data revealed a negative correlation between FANCE expression and the macrophage markers CD68, CD14,and CD206 (Fig. 5B). This correlation was mirrored in the IHC staining of OSCC tumor tissues, where decreased FANCE expression was associated with increased expression of macrophage markers (Fig. 5C). These findings indicate that FANCE expression plays a crucial role in modulating the TME in OSCC, influencing both the infiltration of immune cells and the overall immunological landscape of the tumor.

Integrated analyses highlight the complex role of FANCE in the OSCC TME, influencing not only immune cell infiltration but also the balance between immunosuppressive and antitumor immune responses. The findings suggest that FANCE may serve as a potential therapeutic target for modulating the TME, potentially enhancing the efficacy of immunotherapies in OSCC.

Discussion

In the present study, the role of FANCE in the pathogenesis of OSCC was investigated, and insights into its function in tumor biology and potential as a diagnostic marker were revealed. Bioinformatics analysis of a TCGA dataset revealed an association between enhanced expression of FANCE in tumor tissues and poor survival in patients with OSCC. Machine learning and immune microenvironment analyses enriched comprehension of the role of FANCE in tumor biology. Functional assays indicated that FANCE knockdown inhibited OSCC cell proliferation and migration, confirming its role in oncogenic processes. GSEA showed negative enrichment scores for FANCE, linking it to immune pathways. Correlation analysis identified significant negative associations between FANCE expression and immune checkpoint genes. IHC staining revealed a negative association between FANCE and the immune markers CD14, CD206 and CD68. Collectively, these findings enhanced understanding of the pathophysiology of OSCC and emphasized the multifaceted involvement of FANCE in tumor progression and its interaction with the immune environment.

The findings of the present study demonstrated the enhanced expression of FANCE in OSCC tissues in the TCGA dataset. This convergence underscores the potential oncogenic role of FANCE in OSCC and suggests that its enhanced expression could serve as a reliable and reproducible biomarker. These data contribute to accumulating evidence implicating FANCE in the development of OSCC. Previous in-depth evaluations of robust datasets have provided a solid foundation for understanding of the function of FANCE in diseases including esophageal cancer, hepatocellular carcinoma, breast/ovarian and lung cancer, uterine sarcoma, primary ovarian insufficiency, and common variable immunodeficiency, which mitigates concerns arising from the limitations of the analyzed dataset. Acknowledging the need for integrated bioinformatics and clinical studies, ongoing investigation will further elucidate the clinical application of FANCE in the prognosis and

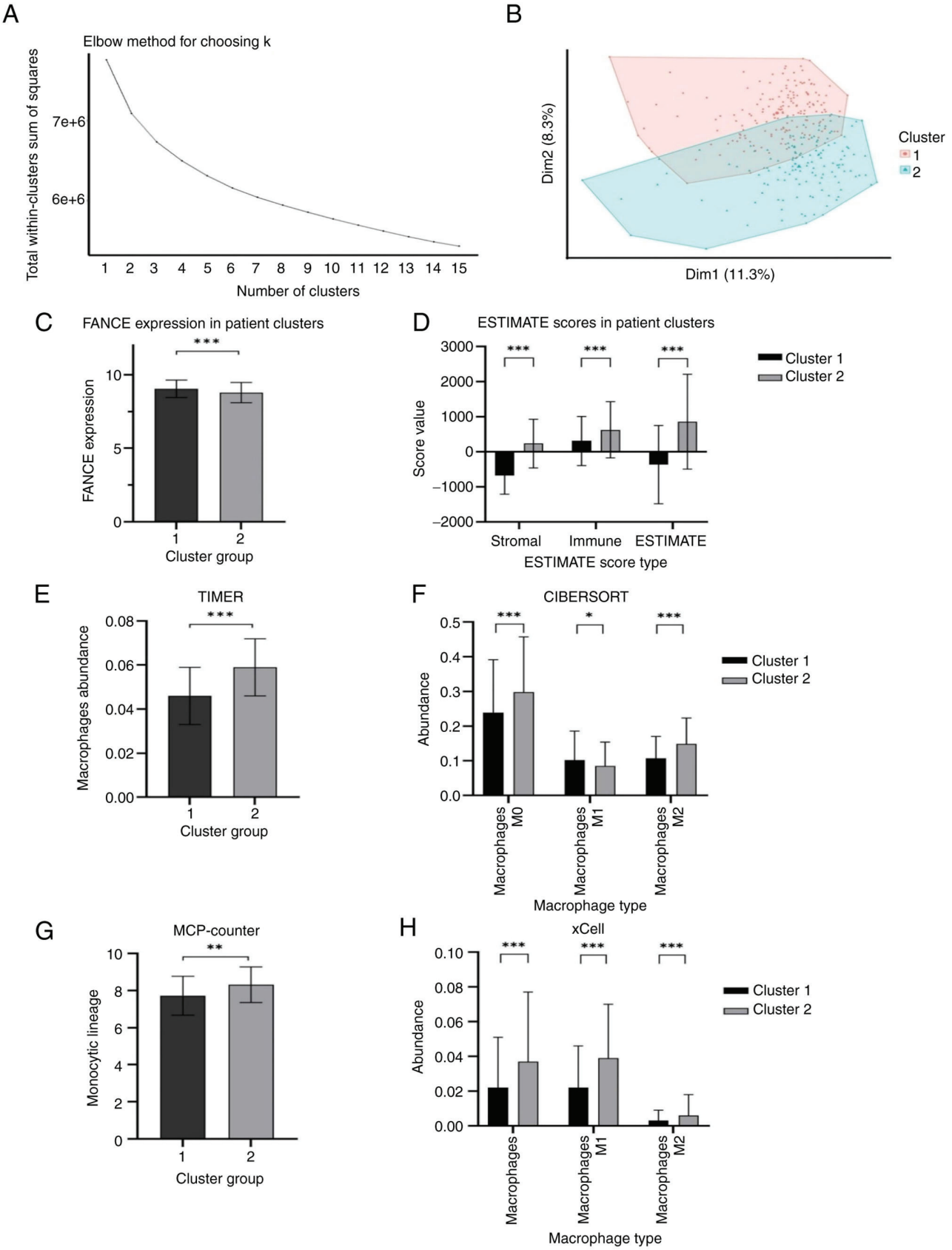

Figure 3. Integrated cluster analysis of samples from patients with OSCC. Statistical analysis was performed using the two-tailed unpaired student's t-tests, and data are presented as the mean ± SD. (A) Elbow method identifying k=2 as the optimal cluster number. (B) k-means clustering on the first two principal components. (C) Box plot of FANCE expression levels in two OSCC subgroups (***P<0.001). (D) Bar chart of TME scores comparing Cluster 1 and 2, (***P<0.001). (E) TIMER analysis shows macrophage abundances for Cluster 1 and Cluster 2. (F) CIBERSORT analysis presents macrophage abundances for Cluster 1 and Cluster 2 across Macrophages M0, M1, and M2 types, with indicated statistical significance (*P<0.05, ***P<0.001). (G) MCP-counter analysis displays monocyte lineage scores for macrophages in Cluster 1 and Cluster 2, with indicated statistical significance (**P<0.01). (H) xCell analysis depicts macrophage abundances for Cluster 1 and Cluster 2 across Macrophages, M1, and M2 types. ***P<0.001). FANCE, Fanconi anemia complementation group E; OSCC, oral squamous cell carcinoma; TME, tumor microenvironment; MCP, Microenvironment Cell Populations.

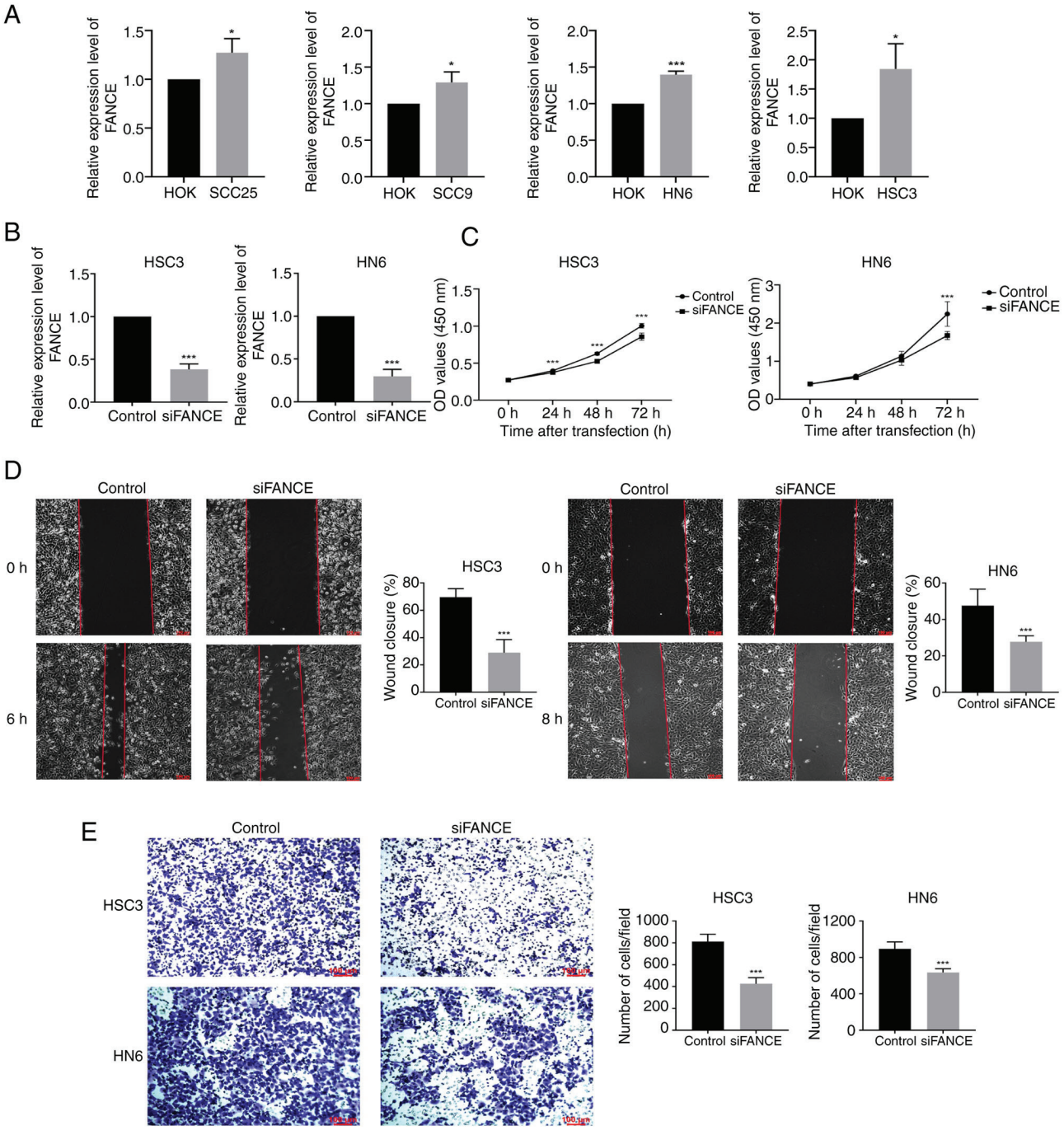

Figure 4. Knockdown of FANCE inhibits the cell proliferation and migration. (A) The FANCE expression levels in HOK and OSCC cells (SCC25, SCC9, HN6 and HSC3 cells) were quantified using RT-qPCR. (B) The FANCE knockdown efficiency was quantified by RT-qPCR. (C) CCK-8 assays were performed using control and FANCE knockdown cells. (D) Wound healing assays were performed using control and FANCE knockdown cells. (E) Transwell migration assays were performed using control and FANCE knockdown cells. The migrated cell number was quantified. Data were presented as the mean ± SD from three independent experiments. *P<0.05, ***P<0.001, two-tailed unpaired student's t-test (scale bars, 100 μm). FANCE, Fanconi anemia complementation group E; OSCC, oral squamous cell carcinoma.

therapy of OSCC. The correlation between FANCE expression and immune cell markers revealed by IHC staining is a qualitative assessment supported by similar methodologies used in other studies, following a well-established approach (15,16). This method is recognized for its effectiveness in illustrating the complex dynamics within the tumor microenvironment (7). Notably, across multiple OSCC tumor samples, an association between decreased FANCE expression and increased expression of macrophage markers (CD68, CD14, CD206) was consistently observed. Although these observations were made through microscopic examination rather than statistical analysis, the consistency of this pattern across the samples in the present study adds robustness to the conclusions.

Unsupervised learning was used to segment the OSCC dataset, initially based on overall gene expression profiles rather than FANCE expression alone. This approach allowed the discovery of significant differences in FANCE expression between clusters, which became a key entry point for

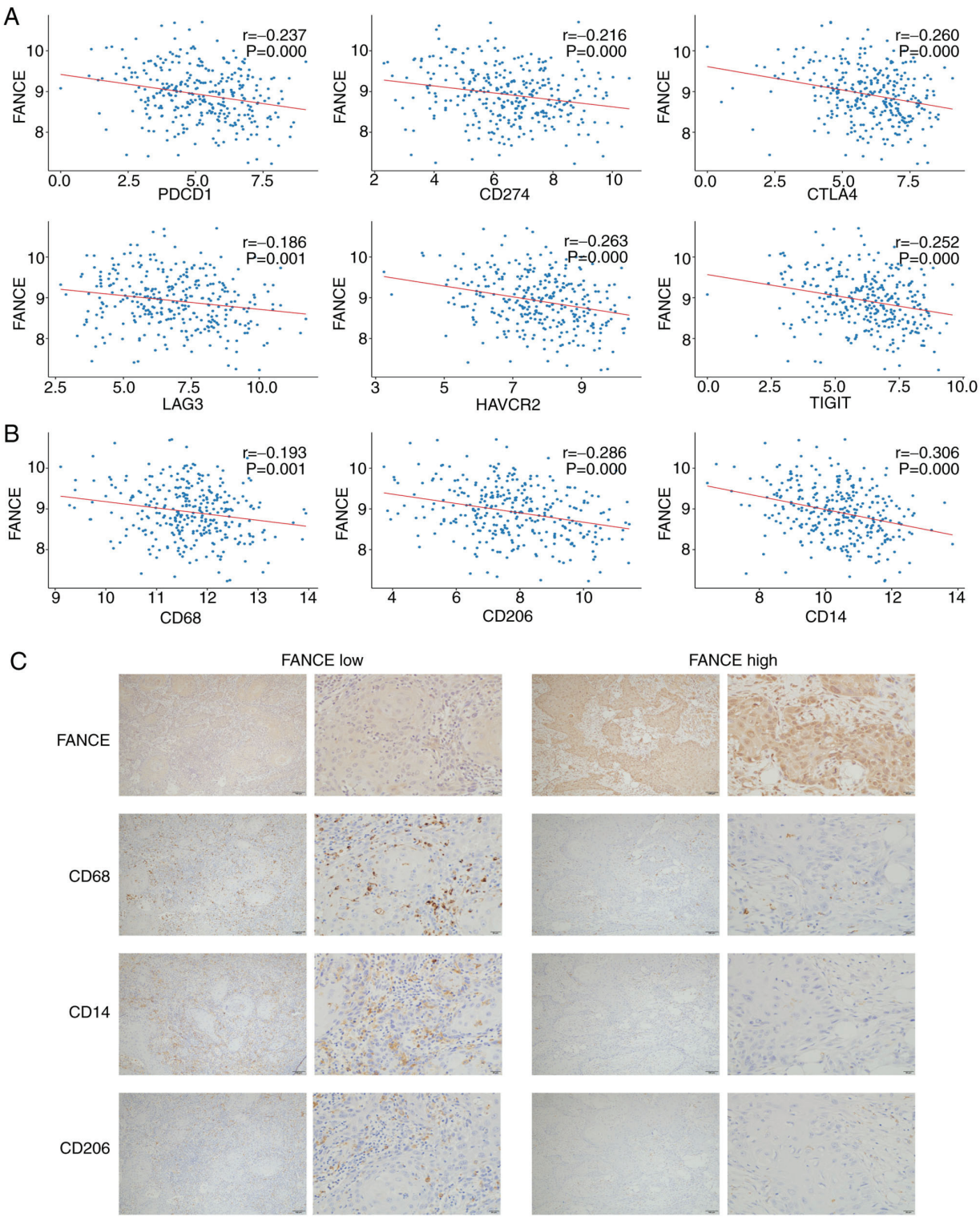

Figure 5. FANCE expression modulates the OSCC tumor microenvironment. (A) Scatter plots demonstrating the negative correlation between FANCE expression and the expression of immune checkpoint genes (PDCD1, CD274, CTLA4, LAG3, HAVCR2 and TIGIT) in OSCC. Each plot includes the Pearson correlation coefficient (r) and P-value indicating statistical significance, with all P≤0.001. (B) Correlation between FANCE and OSCC macrophage markers (CD68, CD14 and CD206) based on TCGA data analysis. Pearson correlation coefficients are shown for each association. All P≤0.001. (C) Immunohistochemical staining of FANCE, CD68, CD14 and CD206 in OSCC tissues. Representative images are shown demonstrating the inverse association between FANCE expression and macrophage markers (scale bars, 100 and 20 μm, respectively). FANCE, Fanconi anemia complementation group E; OSCC, oral squamous cell carcinoma; TCGA, The Cancer Genome Atlas; PDCD1, programmed Cell Death 1; CD274, Cluster of Differentiation 274; CTLA4, Cytotoxic T-Lymphocyte-Associated Protein 4; LAG3, Lymphocyte Activation Gene 3; HAVCR2, Hepatitis A Virus Cellular Receptor 2; TIGIT, T Cell Immunoglobulin and ITIM Domain.

exploring the complex roles of FANCE across molecular subtypes. Given the high heterogeneity of OSCC, this method provided a broader perspective on the role of FANCE, beyond just its expression levels, and helped avoid confirmation bias. The k-means clustering (11,12) revealed distinct molecular subtypes, enabling the detection of subtle but meaningful

FANCE expression differences. These findings not only highlight the intricate interplay between FANCE and the OSCC microenvironment but also lay the groundwork for subsequent functional analyses, allowing for a more nuanced understanding of the role of FANCE in the molecular landscape of OSCC. Although the differences in FANCE expression between the two groups may not appear striking, they are statistically significant, attributed to the large sample size that allows subtle variations to reach significance. This approach reduces the risk of confirmation bias and provides a broader perspective on the complex interplay between FANCE expression and the OSCC microenvironment.

Immune cell infiltration was analyzed using MCP-counter (12), xCell (17), CIBERSORT (18) and TIMER (17) algorithms, each offering a comprehensive perspective on macrophage infiltration. MCP-counter and xCell assessments are based on marker genes of specific cell types, thus accurately mapping distribution and abundance of different immune cell types within samples (17). The CIBERSORT and TIMER methods used a deconvolution-based approach that evaluates samples as mixtures of various immune cells. They can precisely deduce the proportion and expression of each immune cell type *via* complex computational models (19). Although the present analysis reveals some discrepancies, particularly in M1 macrophage abundance between CIBERSORT and xCell, these differences underscore the importance of cross-validating results to ensure robust conclusions. This discrepancy likely arises from inherent differences in the reference gene sets and statistical models used by the two algorithms, which could affect their sensitivity and specificity in detecting certain immune cell types. Notably, the observed differences in macrophage abundance between the molecular subtypes identified through clustering suggest that FANCE could be involved in modulating the immune microenvironment across different OSCC subtypes. While these findings are preliminary, they provide a foundation for further investigation into the role of FANCE in OSCC. Additionally, these insights may guide the selection of appropriate markers for subsequent IHC experiments, thereby helping to clarify the role of FANCE within the broader immunological landscape of OSCC.

The GSEA highlights the multifaceted role of FANCE in OSCC, linking its influence on immune pathways with broader biological processes, including cell growth and migration. While the exploration of the effects of FANCE on cell proliferation and migration and its impact on the TME initially seemed like separate investigations, the integrated approach reveals that these processes may be interconnected. Specifically, the negative enrichment of gene sets associated with immune regulation, such as systemic lupus erythematosus and asthma, suggests that FANCE may normally suppress these pathways. Upon downregulation of FANCE, this suppression could be lifted, potentially activating immune responses that influence tumor behavior, including proliferation and migration. Furthermore, the observed negative correlation between FANCE expression and immune checkpoint genes indicates that FANCE might play a role in modulating the tumor microenvironment, which could affect immune evasion and tumor aggressiveness. These findings underscore the complex role of FANCE in OSCC, not only in regulating cellular behaviors but also in shaping the immune landscape, reinforcing the value of this integrated approach.

The functional assays of the present study provided a compelling account of the role of FANCE in OSCC, as knockdown of FANCE significantly inhibited cell proliferation and migration. These findings support the canonical role of FANCE in DNA repair and cellular stability, suggesting that its deregulation could promote oncogenesis (20,21). While the results of the present study demonstrate a clear impact on cell viability and behavior, the specific mechanisms through which FANCE contributes to these phenotypical changes in OSCC remain unclear. Further investigation is warranted to explore the interplay between FANCE activity and other cellular pathways such as p53 signaling and apoptosis. Additionally, the present bioinformatics analyses, including GSEA and immune checkpoint analysis, highlight the broader impact of FANCE on the tumor microenvironment, suggesting a link between FANCE expression and immune evasion mechanisms. These findings also align with previous literature that implicates FANCE in cancer progression (3,4,6,7,22-24), supporting its consideration as a potential therapeutic target. However, the varying results across different studies reflect the complexity of the role of FANCE in cancer biology, underscoring the importance of a nuanced and carefully tailored approach when evaluating FANCE as a target in clinical settings (25,26).

The significant negative correlation between the expression of FANCE and CD68 in OSCC demonstrates its potential immunomodulatory role, particularly in influencing the infiltration of proinflammatory M1 macrophages within the TME (27). Antitumorigenic M1 macrophages are typically associated with an improved prognosis of cancer (28), and their negative correlation with enhanced FANCE expression suggests a shift towards an immunosuppressive and tumor-promoting microenvironment (6). A negative correlation between FANCE and CD14 and CD206 also indicated initial macrophage activation and an M2 phenotype transition (29,30), respectively. Nevertheless, these preliminary findings align with TCGA analyses of patients in the cBioPortal database (6,7), suggesting a consistent negative correlation between FANCE and macrophage markers. Cross-validation using a public genomic database supports the relevance of the present findings and suggests their applicability to a broader range of OSCC. Elucidating the mechanistic link between FANCE and macrophage polarization is crucial for developing strategies to manipulate the tumor immune microenvironment and enhance the efficacy of immunotherapy in patients with OSCC. Further studies are required to elucidate the precise regulatory function of FANCE and its potential as a therapeutic target.

The present study contributes significantly to the understanding of the functional role of FANCE in OSCC. The results derived from cell lines and retrospective data may not completely mimic the complexity of tumor biology *in vivo* (31). Thus, further investigation is required to validate these findings through clinical trials and models *in vivo* to assess the therapeutic viability of targeting FANCE. Future studies to elucidate details of the molecular mechanisms of FANCE in tumorigenesis and tumor immunity are warranted. Investigating FANCE interactions with other DNA repair

pathways and its impact on OSCC immunogenicity might lead to novel therapeutic targets and the refinement of current treatment paradigms. Furthermore, the integration of FANCE-associated research into advancements in precision medicine may enhance patient management and improve OSCC outcomes.

The present study advances the understanding of the role of FANCE in OSCC, but several limitations must be acknowledged. Firstly, the present research primarily relies on retrospective clinical data and *in vitro* experiments, which, while providing valuable insights, do not fully capture the complexity of OSCC *in vivo*. Although the present study focused on extensive clinical data from a public database, offering a direct reflection of the human condition, animal studies are crucial for validating these findings in a more physiologically relevant context. Additionally, while the present study concentrated on the role of FANCE within the tumor immune microenvironment, its involvement in DNA repair pathways and potential impact on therapy resistance require further exploration. Future endeavors will aim plan to conduct animal studies that complement the current findings and deepen the understanding of the role of FANCE in OSCC. These future directions will help refine therapeutic strategies and contribute to more personalized treatment approaches, ultimately improving patient outcomes.

In conclusion, the results of the present study demonstrated that FANCE is upregulated in OSCC and is correlated with poor survival. Furthermore, FANCE participates in oncogenesis by influencing OSCC cell proliferation and migration. With the help of machine learning clustering and immune infiltration analysis, it was demonstrated that FANCE also plays crucial roles in modulating the immune microenvironment. Overall, this multi-dimensional evidence underlines the potential of FANCE as a therapeutic target for treating OSCC.

Acknowledgements

Not applicable.

Funding

The present research was supported by The Basic Research Program of Shenzhen Innovation Council (grant no. JCYJ20210324110014037), Shenzhen Clinical Medical Research Center for Oral Diseases (grant no. 202106171707 45001-SCRC202201001) and Shenzhen High-level Hospital Construction Fund, Peking University Shenzhen Hospital Scientific Research Fund (grant no. KYQD2023253).

Availability of data and materials

The data generated in the present study may be requested from the corresponding author.

Authors' contributions

BL designed the experiments and drafted the manuscript. YC, YL, XL and JZ conducted the experiments. BL, HY, YS and YC conducted statistical analysis. HY and YS contributed to the study conception, design and interpretation. BL, HY and YS confirm the authenticity of all the raw data. All authors have read and approved the final version of the manuscript.

Ethics approval and consent to participate

The study was conducted according to the Declaration of Helsinki. Human sample collection was approved by the Ethical Committee of the Peking University Shenzhen Hospital (Shenzhen, China; approval no. 2023-177). Written informed consent was obtained from all participants, and the consent forms were collected and stored in accordance with the ethical standards of the institution.

Patient consent for publication

Not applicable.

Competing interests

The authors declare that they have no competing interests.

References

1. Alkire BC, Bergmark RW, Chambers K, Cheney ML and Meara JG: Head and neck cancer in South Asia: Macroeconomic consequences and the role of surgery. Lancet 385 Suppl 2: S56, 2015.
2. Chi AC, Day TA and Neville BW: Oral cavity and oropharyngeal squamous cell carcinoma-an update. CA Cancer J Clin 65: 401-421, 2015.
3. Gordon SM, Alon N and Buchwald M: FANCC, FANCE, and FANCD2 form a ternary complex essential to the integrity of the Fanconi anemia DNA damage response pathway. J Biol Chem 280: 36118-36125, 2005.
4. Zheng C, Ren Z, Chen H, Yuan X, Suye S, Yin H and Fu C: Reduced FANCE confers genomic instability and malignant behavior by regulating cell cycle progression in endometrial cancer. J Cancer 14: 2670-2685, 2023.
5. Taniguchi T, Tischkowitz M, Ameziane N, Hodgson SV, Mathew CG, Joenje H, Mok SC and D'Andrea AD: Disruption of the Fanconi anemia-BRCA pathway in cisplatin-sensitive ovarian tumors. Nat Med 9: 568-574, 2003.
6. Lin B, Li H, Zhang T, Ye X, Yang H and Shen Y: Comprehensive analysis of macrophage-related multigene signature in the tumor microenvironment of head and neck squamous cancer. Aging (Albany NY) 13: 5718-5747, 2021.
7. Zhou Z, Yin H, Suye S, He J and Fu C: Pan-cancer analysis of the prognostic and immunological role of Fanconi anemia complementation group E. Front Genet 13: 1024989, 2023.
8. Del Valle J, Rofes P, Moreno-Cabrera JM, López-Dóriga A, Belhadj S, Vargas-Parra G, Teulé À, Cuesta R, Muñoz X, Campos O, *et al*: Exploring the role of mutations in fanconi anemia genes in hereditary cancer patients. Cancers (Basel) 12: 829, 2020.
9. George M, Solanki A, Chavan N, Rajendran A, Raj R, Mohan S, Nemani S, Kanvinde S, Munirathnam D, Rao S, *et al*: A comprehensive molecular study identified 12 complementation groups with 56 novel FANC gene variants in Indian Fanconi anemia subjects. Hum Mutat 42: 1648-1665, 2021.
10. Snyder ER, Ricker JL, Chen Z and Waes CV: Variation in cisplatinum sensitivity is not associated with Fanconi Anemia/BRCA pathway inactivation in head and neck squamous cell carcinoma cell lines. Cancer Lett 245: 75-80, 2007.
11. Bello-Orgaz G, Menendez HD and Camacho D: Adaptive k-means algorithm for overlapped graph clustering. Int J Neural Syst 22: 1250018, 2012.
12. Zhang Z, Pan Q, Ge H, Xing L, Hong Y and Chen P: Deep learning-based clustering robustly identified two classes of sepsis with both prognostic and predictive values. EBioMedicine 62: 103081, 2020.
13. Schmittgen TD and Livak KJ: Analyzing real-time PCR data by the comparative C(T) method. Nat Protoc 3: 1101-1108, 2008.

14. Song L: A possible approach for stem cell gene therapy of Fanconi anemia. Curr Gene Ther 9: 26-32, 2009.
15. Zaki MYW, Alhasan SF, Shukla R, McCain M, Laszczewska M, Geh D, Patman GL, Televantou D, Whitehead A, Maurício JP, *et al*: Sulfatase-2 from cancer associated fibroblasts: An environmental target for hepatocellular carcinoma? Liver Cancer 11: 540-557, 2022.
16. Wang X, Wang J, Zhao J, Wang H, Chen J and Wu J: HMGA2 facilitates colorectal cancer progression via STAT3-mediated tumor-associated macrophage recruitment. Theranostics 12: 963-975, 2022.
17. Aran D, Hu Z and Butte AJ: xCell: Digitally portraying the tissue cellular heterogeneity landscape. Genome Biol 18: 220, 2017.
18. Newman AM, Liu CL, Green MR, Gentles AJ, Feng W, Xu Y, Hoang CD, Diehn M and Alizadeh AA: Robust enumeration of cell subsets from tissue expression profiles. Nat Methods 12: 453-457, 2015.
19. Chen B, Khodadoust MS, Liu CL, Newman AM and Alizadeh AA: Profiling tumor infiltrating immune cells with CIBERSORT. Methods Mol Biol 1711: 243-259, 2018.
20. Takahashi J, Masuda T, Kitagawa A, Tobo T, Nakano Y, Abe T, Ando Y, Kosai K, Kobayashi Y, Matsumoto Y, *et al*: Fanconi anemia complementation group E, a DNA repair-related gene, is a potential marker of poor prognosis in hepatocellular carcinoma. Oncology 100: 101-113, 2022.
21. Polito D, Cukras S, Wang X, Spence P, Moreau L, D'Andrea AD and Kee Y: The carboxyl terminus of FANCE recruits FANCD2 to the Fanconi Anemia (FA) E3 ligase complex to promote the FA DNA repair pathway. J Biol Chem 289: 7003-7010, 2014.
22. Gille JJ, Floor K, Kerkhoven L, Ameziane N, Joenje H and de Winter JP: Diagnosis of fanconi anemia: Mutation analysis by multiplex ligation-dependent probe amplification and PCR-based sanger sequencing. Anemia 2012: 603253, 2012.
23. Philip PA, Azar I, Xiu J, Hall MJ, Hendifar AE, Lou E, Hwang JJ, Gong J, Feldman R, Ellis M, *et al*: Molecular characterization of KRAS wild-type tumors in patients with pancreatic adenocarcinoma. Clin Cancer Res 28: 2704-2714, 2022.
24. Pillonetto DV, Piovezan BZ, Nichele S, Lima ACM, Pasquini R, Pereira NF and Bonfim C: Investigation of mutations in Fanconi anemia genes and malignancy predisposition in Brazilian patients. Int J Lab Hematol 45: 82-89, 2023.
25. Fu C, Begum K, Jordan PW, He Y and Overbeek PA: Dearth and delayed maturation of testicular germ cells in fanconi anemia E mutant male mice. PLoS One 11: e0159800, 2016.
26. Fu C, Begum K and Overbeek PA: Primary ovarian insufficiency induced by fanconi anemia E mutation in a mouse model. PLoS One 11: e0144285, 2016.
27. Ferrisse TM, de Oliveira AB, Palacon MP, Silva EV, Massucato EMS, de Almeida LY, Léon JE and Bufalino A: The role of CD68+ and CD163+ macrophages in immunopathogenesis of oral lichen planus and oral lichenoid lesions. Immunobiology 226: 152072, 2021.
28. Mantovani A, Marchesi F, Malesci A, Laghi L and Allavena P: Tumour-associated macrophages as treatment targets in oncology. Nat Rev Clin Oncol 14: 399-416, 2017.
29. Jayasingam SD, Citartan M, Thang TH, Mat Zin AA, Ang KC and Ch'ng ES: Evaluating the polarization of tumor-associated macrophages into M1 and M2 phenotypes in human cancer tissue: Technicalities and challenges in routine clinical practice. Front Oncol 9: 1512, 2020.
30. Schraufstatter IU, Zhao M, Khaldoyanidi SK and Discipio RG: The chemokine CCL18 causes maturation of cultured monocytes to macrophages in the M2 spectrum. Immunology 135: 287-298, 2012.
31. Kimura Y: New anticancer agents: In vitro and in vivo evaluation of the antitumor and antimetastatic actions of various compounds isolated from medicinal plants. In Vivo 19: 37-60, 2005.